Collective flow in heavy-ion collisions for $E_{\rm lab} = 1$–160 GeV/nucleon

V. N. Russkikh[1,2,*] and Yu. B. Ivanov[1,2,†]
[1]*Gesellschaft für Schwerionenforschung mbH, Planckstrasse 1, D-64291 Darmstadt, Germany*
[2]*Kurchatov Institute, Kurchatov Square 1, Moscow, RU-123182, Russia*
(Received 5 June 2006; published 15 September 2006)

Collective transverse flow in heavy-ion collisions at incident energies $E_{\rm lab} \simeq (1$–$160)A$ GeV is analyzed within the model of three-fluid dynamics (3FD). Simulations are performed with a purely hadronic equation of state (EoS). At the AGS energies the flow turns out to be sensitive to the stopping power of nuclear matter rather than only to the stiffness of the EoS. When the stopping power is fixed to reproduce other observables, the flow data favor more and more soft EoS with the incident energy rise, which can be associated with "a transition from hadronic to string matter" reported in the hadron-string-dynamics (HSD) model. Problems, which are met in simultaneous reproduction of directed and elliptic flows within the 3FD, suggest that the transverse flow is very sensitive to the character of the transverse-momentum nonequilibrium at the initial stage of collision. Arguments in favor of the early-stage nature of the flow observable are put forward. This suggests that the flow (especially the directed one) is determined by early-stage evolution of the collision rather than the freeze-out stage.

DOI: 10.1103/PhysRevC.74.034904 PACS number(s): 24.10.Nz, 25.75.Ld, 21.65.+f

I. INTRODUCTION

Interest in nucleus-nucleus collisions at incident energies $E_{\rm lab} \simeq (10$–$40)A$ GeV has been recently revived, since the highest baryon densities [1–3] and highest relative strangeness [4,5] at moderate temperatures are expected in this energy range. The onset of deconfinement is also expected in this domain. In particular, the energy-scan CERN Super Proton Synchrotron (SPS) program [6] is dedicated to the search for the onset of deconfinement in heavy-ion collisions. Moreover, a critical end point [7] of the QCD phase diagram may be accessible in these reactions [8,9]. The above expectations motivated the project of the new accelerator Facility for Antiproton and Ion Research (FAIR) at GSI [10], the heavy-ion program of which is precisely dedicated to studying dense baryonic matter with the emphasis on the onset of deconfinement and the critical end point. The future SPS [11] and BNL Relativistic Heavy Ion Collider (RHIC) [12] programs are also devoted to the same problems.

In Refs. [3,13] we introduced a three-fluid dynamical (3FD) model that is suitable for simulating heavy-ion collisions in the range from BNL Alternating Gradient Synchrotron (AGS) to SPS energies, which overlaps the energy range of the future FAIR. We have started simulations [3] with the purely hadronic equation of state (EoS) [14] to see how well the available data from AGS and SPS can be understood without involving the concept of deconfinement. This EoS should serve as a reference point for simulations involving more sophisticated EoS's including the phase transition.

With this simple hadronic EoS we succeeded in reasonably reproducing a great body of experimental data in the incident energy range $E_{\rm lab} \simeq (1$–$160)A$ GeV. The list includes rapidity distributions, transverse-mass spectra, and multiplicities of various hadrons. However, we also found certain problems. In particular, we failed to describe the transverse flow at $E_{\rm lab} \geqslant 40A$ GeV.

One of the main conclusions of Ref. [3] is that in order to judge the relevance of a particular EoS the whole available set of data should be analyzed in a wide incident energy range with the same fixed parameters of the model. Indeed, for almost any particular portion of the data the parameters of the model can be tuned in such a way that the model reasonably reproduces the data. At the same time the reproduction of the whole set of available data with the same model parameters is far from always being possible. In Ref. [3] we performed still fragmentary analysis of data owing to constraints of the Framework of a single paper. Therefore in the present paper we continue our analysis of a particular subset of the data concerning collective flow in nuclear collisions, based on the set of model parameters fixed in Ref. [3]. According to our preliminary results [3], this subset is the most problematic for the purely hadronic EoS we use.

The collective transverse flow is formed at the early (compression) stage of the collisions and hence reveals the early pressure gradients in the evolving nuclear matter. The harder the EoS is, the stronger the pressure that is developed. Thus the flow reflects the stiffness of the nuclear EoS. The collective-flow observable has been extensively exploited to obtain information on the EoS [15–51]. In particular, it was expected that the transition to the quark-gluon phase would result in significant reduction of the directed flow [52] (the so-called softest-point effect), since the pressure in the quark-gluon phase is lower than that in the hadronic phase. Calculations within conventional (one-fluid) hydrodynamics [30] indicated the near disappearance of the flow at the onset of the first-order phase transition. However, the nuclear finite stopping power essentially weakens this effect [34,42]. In the present paper we discuss the transverse flow in terms of the stiffness of the nuclear EoS and the stopping power achieved in the collision.

*Electronic address: russ@ru.net
†Electronic address: y.ivanov@gsi.de

At present there are quite systematic collective-flow data, for both directed and elliptic transverse flows, at AGS [53–59] and SPS [60–63] energies. We confine our present discussion to the flow of nonstrange probes, i.e., nucleons and pions. Recent analysis of this set of data was done in Ref. [45] with emphasis on the momentum dependence of nuclear forces. This was done within the JAM model [64] combined with a covariant prescription of mean fields (RQMD/S) [65] with the emphasis on the momentum dependence of nuclear forces. We analyze the same data but within the hydrodynamic approach.

II. THREE-FLUID DYNAMICS MODEL

A direct way to address thermodynamic properties of the matter produced in these reactions consists in application of hydrodynamic simulations to nuclear collisions. However, finite nuclear stopping power, revealing itself at high incident energies, makes the collision dynamics nonequilibrium and prevents us from application of conventional hydrodynamics, especially at the initial stage of the reaction. Since the resulting nonequilibrium is quite strong, introduction of viscosity and thermal conductivity does not help to overcome this difficulty, because by definition they are suitable for weak nonequilibrium. A possible way out is taking advantage of a multifluid approximation to heavy-ion collisions.

Unlike conventional hydrodynamics, where local instantaneous stopping of projectile and target matter is assumed, a specific feature of the dynamic three-fluid description is a finite stopping power resulting in a counterstreaming regime of leading baryon-rich matter. Experimental rapidity distributions in nucleus–nucleus collisions support this counterstreaming behavior, which can be observed for incident energies between few and 200A GeV. The basic idea of a three-fluid approximation to heavy-ion collisions [3,13] is that at each space-time point $x = (t, \mathbf{x})$ the generally nonequilibrium distribution function of baryon-rich matter, can be represented as a sum of two distinct contributions, $f_{\rm bar}(x, p) = f_{\rm p}(x, p) + f_{\rm t}(x, p)$, initially associated with constituent nucleons of the projectile (p) and target (t) nuclei. In addition, newly produced particles, populating the midrapidity region, are associated with a fireball (f) fluid described by the distribution function $f_{\rm f}(x, p)$. It is assumed that constituents within each distribution are locally equilibrated, both thermodynamically and chemically. This assumption, justifying the term "fluids," relies on the fact that intrafluid collisions are much more efficient in driving a system to equilibrium than interfluid interactions. Therefore the three-fluid approximation is a minimal way to simulate the finite stopping power at high incident energies. Note that both the baryon-rich and the fireball fluids may consist of any type of hadron and/or parton (quarks and gluons), rather than only nucleons and pions.

Our 3FD model [3,13] is a straightforward extension of the two-fluid model with radiation of direct pions [66–68] and the $(2 + 1)$-fluid model [69,70]. We extend the above models in such a way that the created baryon-free fluid (which we call a fireball fluid, following the Frankfurt group) is treated on equal footing with the baryon-rich ones. We allow a certain formation time for the fireball fluid, during which the matter of the fluid propagates without interactions. We assume that the fireball matter quickly becomes thermalized after its formation. The latter approximation is an enforced one, since we deal with the hydrodynamics rather than with kinetics.

The main unknowns of the present simulations can be briefly summarized as follows: an EoS and cross sections. Our goal is to find an EoS that in the best way reproduces the largest body of available observables. The cross sections are equally important. They determine friction forces between fluids and hence the nuclear stopping power. In principle, friction forces are EoS dependent, because medium modifications, providing a nontrivial EoS, also modify cross sections and should be externally supplied with the EoS. However, at present we have at our disposal only a rough estimate of the friction forces [71]. Therefore we have to fit the friction forces to the stopping power observed in proton rapidity distributions.

We have started our simulations [3] with a simple, purely hadronic EoS [14] that involves only a density-dependent mean field providing saturation of cold nuclear matter at normal nuclear density $n_0 = 0.15$ fm^{-3}, and with the proper binding energy -16 MeV; cf. Appendix A. This EoS is a natural reference point for any other more elaborate EoS.

Figure 1 displays the density dependence of the pressure of four versions of this hadronic EoS at zero temperature: hard EoS with incompressibility $K = 380$ MeV, intermediate EoS with $K = 210$ MeV, soft EoS with $K = 130$ MeV, and extrasoft EoS with $K = 100$ MeV. The pressure of the nucleon gas is also presented, indicating the softest EoS within our parametrization. As is seen from Fig. 1, the intermediate EoS with which all the calculations of Ref. [3] were done, and the soft EoS are within the constraint given by Danielewicz *et al.* [44] based on the analysis of the flow of nuclear matter at the AGS incident energies.

Strictly speaking, the constraint region of Ref. [44] is valid for the class of EoS's considered in [44], since the flow essentially depends also on the temperature dependence of the pressure, which is not displayed in Fig. 1. Moreover, since the incompressibility characterizes the EoS only in the vicinity of the bound state, different EoS's with the same incompressibility may differ at higher densities even at zero

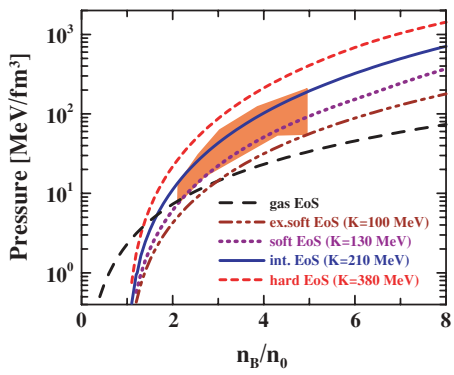

FIG. 1. (Color online) Baryon-density dependence of the pressure at zero temperature for hard ($K = 380$ MeV), intermediate ($K = 210$ MeV), soft ($K = 130$ MeV), extrasoft ($K = 100$ MeV), and gas EoS's. The shaded region is the constraint derived from experimental data in Ref. [44].

temperature. This is the reason that the incompressibility of our intermediate EoS ($K = 210$ MeV) differs from that of the intermediate EoS of Ref. [44] ($K = 300$ MeV), while these two EoS's are very similar at densities higher than $2n_0$. The same applies to soft EoS's: $K = 130$ MeV in our case, and $K = 210$ MeV in Ref. [44]. Of course, values $K = 100$ and 130 MeV are unrealistically small from the point of view of low-energy nuclear physics. However, in simulating heavy-ion collisions we predominantly deal with densities $n \gtrsim 2n_0$. Therefore we should estimate the degree of reasonableness of a EoS precisely in this density region, considering the incompressibility only as label for the EoS.

A comprehensive analysis of the nuclear EoS [72], based on astrophysical data, indicated that the preferable region of Fig. 1 should be slightly shifted to higher pressures. Thus the hard version of our EoS also falls into the region of EoS's that are reasonable from the astrophysical point of view. At the same time, our soft and extrasoft EoS's fall out of this astrophysically acceptable region.

The 3FD model with the intermediate EoS turned out to be able to reasonably reproduce a great body of experimental data [3] in a wide energy range from AGS to SPS. Figure 2 illustrates (and extends) the results of Ref. [3]. The experimental data were compiled in Ref. [73] based on reported experimental results [74–82]. These data slightly differ in the degree of centrality at which they were taken. We, however, performed our calculations for Au+Au collisions at fixed impact parameter $b = 2$ fm for the AGS energies and for Pb+Pb at $b = 2.5$ fm for the SPS energies. The slight irregularity of calculated curves between $\sqrt{s_{NN}} = 4.85$ GeV and $\sqrt{s_{NN}} = 6.27$ GeV (i.e., between $E_{\rm lab} = 10A$ GeV and $E_{\rm lab} = 20A$ GeV) is related to transition to different colliding nuclei at different impact parameters. A poor description of K^+ and Λ yields at low incident energies is not surprising, since our EoS is based on the grand canonical ensemble.

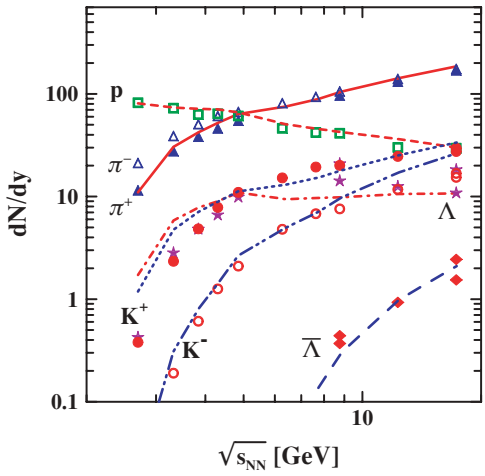

FIG. 2. (Color online) Incident energy dependence of midrapidity yield of various hadrons produced in central nucleus-nucleus collisions. At the AGS energies the 3FD calculations with intermediate EoS ($K = 210$ MeV) were done for Au+Au collisions at impact parameter $b = 2$ fm; at SPS energies, for Pb+Pb at $b = 2.5$ fm. The compilation of experimental data is taken from Ref. [73].

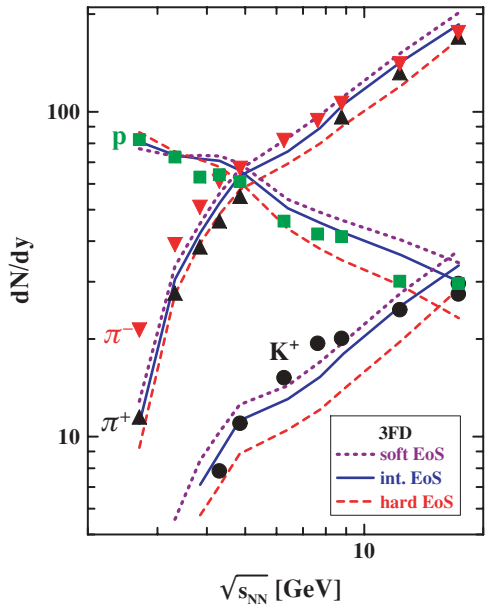

FIG. 3. (Color online) Same as in Fig. 2 but enlarged and for three EoS's displayed in Fig. 1.

Really surprising is the fact that K^- and $\bar{\Lambda}$ yields are still well reproduced at low energies.

In the present paper we also do calculations with hard, soft, and estrasoft EoS's (cf. Fig. 1) in order to study effects of the EoS stiffness. Changes introduced by these hard and soft EoS's are presented in Fig. 3. As is seen, the intermediate EoS is indeed preferable in overall reproduction of the data.

To study the effect of nuclear stopping power on the transverse flow, we also do calculations within the conventional one-fluid dynamics (1FD), for which we have a separate code.

III. DIRECTED FLOW

The conventional transverse-momentum flow of an a species is defined as [83]

$$\langle p_x^{(a)} \rangle (y) = \frac{\int d^2 p_T \, p_x E dN_a/d^3 p}{\int d^2 p_T \, E dN_a/d^3 p}, \qquad (1)$$

where p_x is the transverse momentum of a particle in the reaction plane, $E dN_a/d^3 p$ is the momentum distribution of a hadrons, which takes due account of feeddown from resonance decays, and integration runs over the transverse momentum p_T.

In Figs. 4–6 the comparison with Bevalac and AGS data on the directed flow of protons [21,55,58] and nucleons [21,55] is presented. Under "nucleon" data we mean the combined flow of identified protons and light nuclear fragments [21,55]. In fact, we compute $\langle p_x \rangle$ of so-called primordial nucleons, which later may coalesce, forming light fragments. In view of this, the comparison with the nucleon data is preferable for our model, since it avoids additional assumptions of coalescence. In the case of $E_{\rm lab} = 10.5A$ GeV (cf. Fig. 6), agreement with nucleon data indeed seems to be better than that with identified-proton data. Since experimentally the sideward flow is observed for

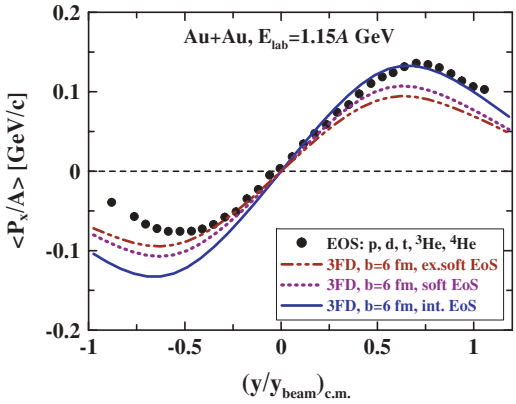

FIG. 4. (Color online) Directed flow of nucleons as a function of rapidity for mid-central Au+Au collisions at $E_{\rm lab} = 1.15A$ GeV. The 3FD results at $b = 6$ fm are presented for three EoS's. The data are from Ref. [21].

mid-central collisions with an average impact parameter of $b = 6$ fm, we restrict our computation to this single impact parameter here.

It is seen that the observed directed flow prefers more and more soft EoS with the incident energy rise. While at $E_{\rm lab} \lesssim 2A$ GeV the intermediate EoS is preferable, even the soft EoS looks too hard at $E_{\rm lab} \gtrsim 8A$ GeV. At $E_{\rm lab} = 8A$ GeV the extrasoft EoS is certainly preferable, while at $E_{\rm lab} = 10.5A$ GeV it is difficult to choose between soft and extrasoft EoS's. However, in Refs. [43,45,48], a rather weak sensitivity of the flow to the stiffness of the EoS was reported. An apparent reason for this disagreement is that in the cited models the EoS becomes effectively softer with incident energy rise. At higher

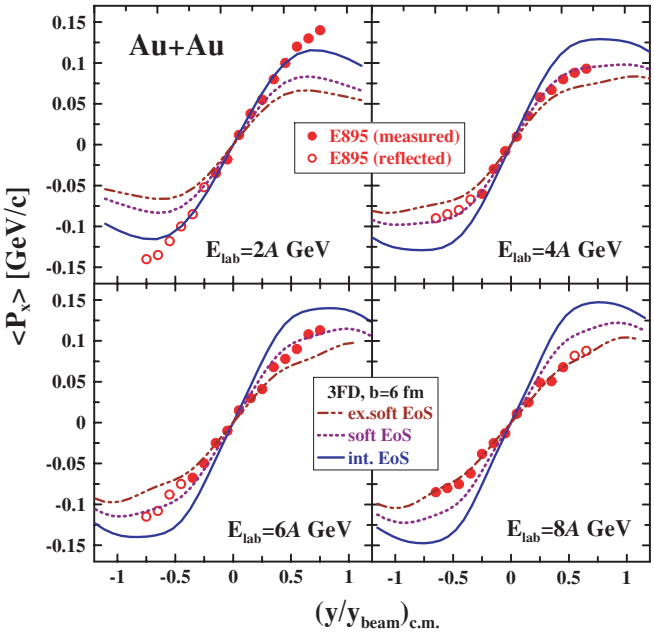

FIG. 5. (Color online) Directed flow of protons as a function of rapidity for mid-central Au+Au collisions at $E_{\rm lab} = 2A$, $4A$, $6A$, and $8A$ GeV. The 3FD results at $b = 6$ fm are presented for three EoS's. The data are from Ref. [58].

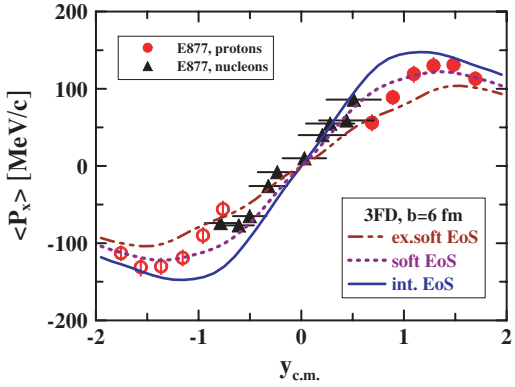

FIG. 6. (Color online) Directed flow of nucleons and protons as a function of rapidity for mid-central Au+Au collisions at $E_{\rm lab} = 10.5A$ GeV. The 3FD calculations with three EoS's are presented for impact parameter $b = 6$ fm. Data are from Ref. [55]. Solid symbols correspond to measured data, open ones are those reflected with respect to the midrapidity point.

incident energies this softening occurs because of gradual (governed by form factors) [43] or abrupt [48] switching off of mean-field interactions, or because more and more initial baryon–baryon collisions at the early collision stage end up in strings that are not affected by the nuclear mean field [45]. Since the mean-field switching off is also accompanied by dominating string excitations in the models of Refs. [43,48], it is possible to summarize this mechanism as "a transition from hadronic to string matter," following Ref. [40]. This early-stage string matter results in effective softening of the EoS.

The flow magnitude is conventionally defined as the slope of directed flow at midrapidity,

$$F_y^{(a)} = \left(\frac{d\langle p_x^{(a)} \rangle}{dy} \right)_{y=y_{\rm c.m.}}. \tag{2}$$

The excitation function of the proton flow magnitude is shown in Fig. 7. This figure summarizes observations made above. In fact, the point at $E_{\rm lab} = 1.15A$ GeV is somewhat misleading. While the differential directed flow is well reproduced at this energy (cf. Fig. 4), the slope is not, because of asymmetry of the data with respect to midrapidity. Note that for a symmetric system such as Au+Au the flow should be antisymmetric with respect to midrapidity. Additionally, Fig. 7 demonstrates that the nuclear stopping power also essentially affects the directed flow. The conventional one-fluid simulations (infinite stopping power) result in essentially stronger flow than it is observed.

At high energies the azimuthal asymmetry is usually characterized by the first coefficients of the Fourier expansion of the azimuthal-angle dependence of the single-particle distribution function, i.e. by the directed flow $v_1 = \langle \cos\phi \rangle$ [84]:

$$v_1^{(a)}(y) = \frac{\int d^2p_T \, (p_x/p_T) \, E dN_a/d^3p}{\int d^2p_T \, E dN_a/d^3p}. \tag{3}$$

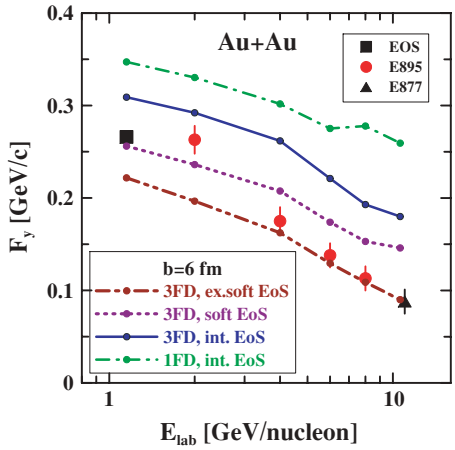

FIG. 7. (Color online) Proton flow magnitude as a function of beam energy for mid-central Au+Au collisions. The 3FD calculations are presented for and $b = 6$ fm. Compilation of the data is from Ref. [58].

Examples of v_1 flow for protons and pions at $E_{\rm lab} = 40A$ and $158A$ GeV are presented in Fig. 8 for mid-central collisions. The 3FD simulations are performed at a fixed impact parameter of $b = 5.6$ fm. Several sets of data, which noticeably differ from one another, are shown in these figures. The standard method [83–85] for evaluating the flow coefficients requires an event-by-event estimate of the reaction plane with which outgoing hadrons correlate. However, this method does not discriminate other sources of correlations, such as those due to global momentum conservation and resonance decays. A new method [86] of n-particle correlations allows us to get rid of these nonflow correlations in extracting v_1 and v_2 from genuine azimuthal correlations.

At these energies the proton v_1 flow, calculated with intermediate and soft EoS's, significantly differs from the data. The experimental data favor extrasoft EoS, which already became preferable at $E_{\rm lab} = 8A$ GeV; cf. Fig. 5. Thus the EoS softening with the incident energy rise stops near the top AGS energy; at higher energies the same extrasoft EoS remains preferable. This fits the observation in Ref. [40] that the "transition from hadronic to string matter," i.e., early-stage softening of the EoS, practically saturates at the top AGS energy. Apparently the early-stage softening of the EoS at SPS energies is the reason for the success of microscopic RQMD [47], UrQMD [48], JAM [45] and HSD [51] models. These models reveal quite soft dynamics at the early stage, since mean fields turn out to be essentially reduced in this energy range.

The lower panels, Fig. 8(b), demonstrate what happens if we further soften the EoS. Slight softening of the extrasoft EoS, i.e., taking $K = 90$ MeV, results in better reproduction of pion v_1, but at the expense of proton flow. The softest EoS, i.e., the gas EoS (cf. Fig. 1) again already contradicts the data, since it produces a wiggle in proton v_1, which is not experimentally observed.

The calculated pion directed flow closely follows the pattern of the proton directed flow, while the pion v_1 data reveal anticorrelation with proton flow. In fact, our pion directed

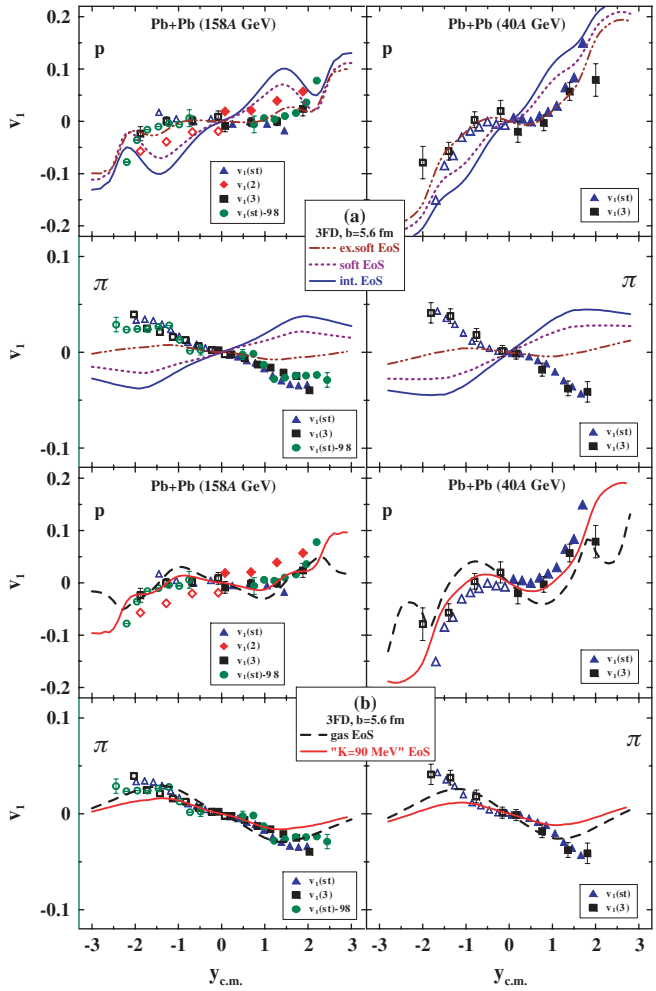

FIG. 8. (Color online) Directed flow of protons (upper panels) and charged pions (lower panels) in mid-central Pb+Pb collisions at $E_{\rm lab} = 158A$ (left panels) and $40A$ (right panels) GeV as a function of rapidity. In the upper block of panels (a) the 3FD calculations at $b = 5.6$ fm are presented for intermediate, soft, and extrasoft EoS's; in the lower block (b), the gas EoS and EoS with $K = 90$ MeV. Experimental data [62] obtained by two different methods are displayed, the standard method [$v(st)$] and the method of n-particle correlations [$v(n)$]. Solid symbols correspond to measured data, while open symbols are those reflected with respect to the midrapidity. Updated data of the NA49 Collaboration [60] [$v(st) - 98$], with acceptance $0.05 < p_T < 0.35$ GeV/c for pions and $0.6 < p_T < 2.0$ Gev/c for protons, are also shown.

flow correlates with the proton directed flow even at lower, AGS energies, instead of anticorrelating. A probable reason for this poor reproduction of pion v_1 is that the fact has been disregarded that a part of the frozen-out particles is shadowed by still hydrodynamically evolving matter. This mechanism of proton-pion anticorrelation was discussed in Refs. [87,88]. In terms of hydrodynamics, this shadowing means that frozen-out particles cannot freely propagate through the region still occupied by the hydrodynamically evolved matter but rather become reabsorbed into the hydrodynamic phase. Apparently the baryon directed flow is less affected by this shadowing. The reason is that the baryon directed flow reveals the collective

flow of matter, since this matter is built mainly of baryons as the most abundant and heavy component of the system. This collective flow is formed mainly at the early stage of the reaction. Baryon rescatterings within this earlier-formed collective flow at later stages do not essentially alter the collective transverse momentum of the matter. At the same time, the pions are more strongly affected by this shadowing, since they are screened by the predominantly baryonic matter, where pions may rescatter or even be absorbed. This can drastically change the pion v_1.

IV. ELLIPTIC FLOW

The elliptic flow, $v_2 = \langle \cos 2\phi \rangle$ [84], is the second coefficient of Fourier expansion of the azimuthal-angle dependence of the single-particle distribution function

$$v_2^{(a)}(y) = \frac{\int d^2p_T \left[\left(p_x^2 - p_y^2\right)/p_T^2\right] E dN_a/d^3p}{\int d^2p_T \, E dN_a/d^3p}. \quad (4)$$

The impact parameter dependence of the proton elliptic flow for Au+Au collisions at energies $E_{\rm lab} = 2A, 4A$, and $6A$ GeV without any cut on the transverse momentum ($p_T > 0$) is presented in Fig. 9. We see that the soft and intermediate

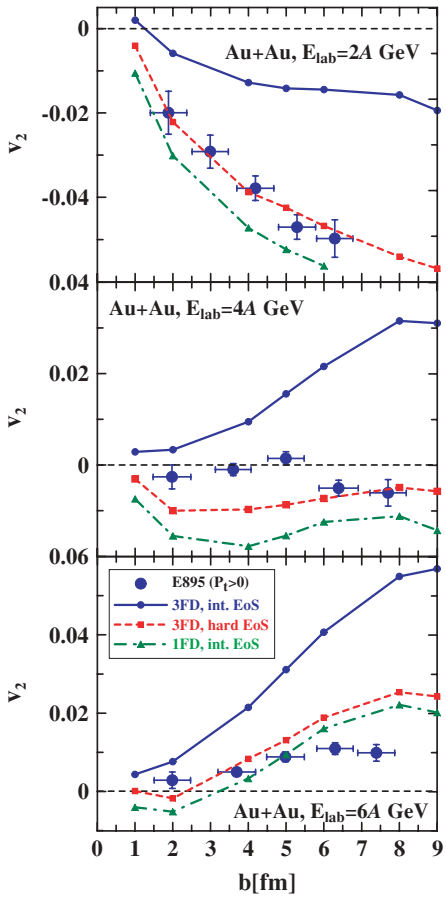

FIG. 9. (Color online) Midrapidity elliptic flow as a function of impact parameter in Au+Au collisions at $E_{\rm lab} = 2A, 4A$ and $6A$ GeV. Experimental data for $p_T > 0$ are from Ref. [54].

EoS's, which are the best in reproducing the directed flow, are completely off the experimental data. At the same time, the hard EoS reasonably reproduces v_2. This observation is similar to that in Refs. [24,44,54]. In Refs. [43,45,51] it was found that a proper momentum dependence in the nuclear mean field is of prime importance for the simultaneous reproduction of the directed and elliptic flows.

The fact that this momentum dependence is vitally important apparently again implies that the initial stage of nuclear collision is essentially nonequilibrium and that the flow is sensitive to this early nonequilibrium in the transverse-momentum distribution. Indeed, even if momentum-dependent forces are present in the model underlying a EoS, in the EoS this momentum dependence is integrated out with the equilibrium momentum distribution. Therefore the in- and out-of-reaction-plane transverse pressures, which are responsible for v_1 and v_2 flows, are tightly interrelated. This prevents the 1FD model from simultaneous reproduction of v_1 and v_2. In the 3FD model these two components of pressure are less tightly interrelated but still do not possess the same degree of freedom as in genuine nonequilibrium, since a superposition of three equilibrium distributions certainly confines the class of possible nonequilibrium momentum configurations. The three-fluid approximation was designed to simulate primarily the transverse-longitudinal anisotropy of the momentum distribution. It was not specially tuned to describe anisotropy within the transverse direction, which is of prime importance for v_2. Apparently the genuine momentum nonequilibrium at the initial stage together with proper momentum dependence in the nuclear mean field is required for simultaneous reproduction of the directed and elliptic flows.

In view of the above said, our intermediate EoS, which is the best in overall reproduction of a large body of other data, can be considered a kind of compromise, allowing to one reproduce orders of magnitude of the directed and elliptic flows simultaneously, within the assumptions of the 3FD model.

Results of 1FD simulations are also presented in Fig. 9. In fact, at energies $E_{\rm lab} = 2A, 4A$, and $6A$ GeV the degree of stopping is already rather high in the 3FD. As is seen from Fig. 10, proton rapidity distributions in 1FD do not differ very much from those in 3FD and from experimental data [75,76]. The same applies to other observables, except flow. The flow exhibits a much harder pattern within the 1FD at the same intermediate EoS (see also Fig. 7) and effectively looks like that for the hard EoS in 3FD.

Available data on the pion elliptic flow at the AGS energies (see Fig. 11) are not very spectacular. They only allow us to estimate the order of magnitude of the v_2 value. As is seen here, the difference between hard and intermediate EoS's is not already that large, and the 1FD result is in the best agreement with the data.

The rapidity dependence of the v_2 flow for protons and pions at $E_{\rm lab} = 40A$ and $158A$ GeV are presented in Fig. 12. Here we see that stiffness of the EoS only weakly affects the result. Even the difference between extremes, i.e., the hard EoS and gas EoS, is quite moderate. The same feature was observed in the JAM simulations [45], but the reason there was different. In Ref. [45] string excitations dominate particle production at early times. These strings are not affected by the

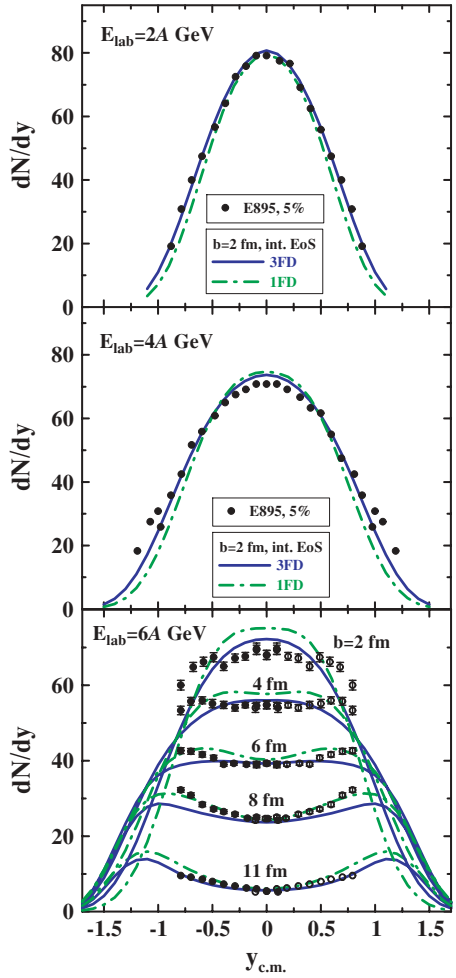

FIG. 10. (Color online) Proton rapidity spectra at AGS energies for various impact parameters. Solid lines correspond to 3FD calculations with intermediate EoS. For comparison the 1FD result with the same EoS is shown by the dotted-dashed line. Experimental points are taken from [75] at 2A and 4A GeV, and [76] at 6A GeV. The percentage indicates the fraction of the total reaction cross section, corresponding to experimentally selected events.

nuclear mean field under the assumption of the JAM model. Therefore the mean-field effects are small at the SPS energies.

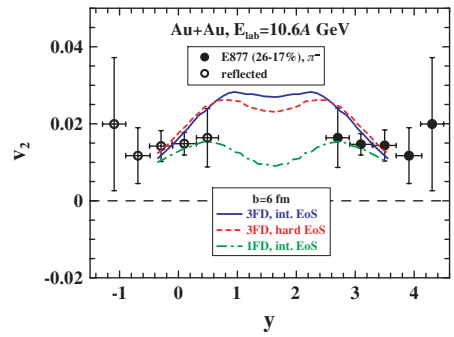

FIG. 11. (Color online) Pion elliptic flow as a function of rapidity in Au+Au collisions at $E_{\rm lab} = 11.5A$ GeV. Experimental data for $p_T > 0$ are from Ref. [56].

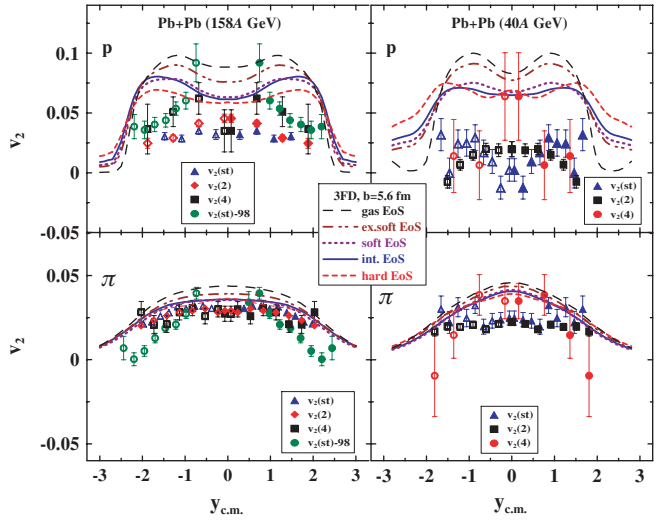

FIG. 12. (Color online) The same as in Fig. 8 but for the elliptic flow.

In our case the mean-field effects (i.e., stiffness of the EoS) are present to the full extent, and nevertheless their effect is small.

The pion elliptic flow at 158A GeV is in surprisingly good agreement with experimental data both in magnitude and shape. However, in spite of the weak dependence on the EoS stiffness, we still essentially overestimate the proton v_2 at both incident energies, 40A and 158A GeV. Moreover, the better we reproduce v_1 (with extrasoft EoS), the worse result we obtain for v_2. This again implies that the nonequilibrium transverse-momentum anisotropy at the initial stage of nuclear collision (now already without serious interplay with momentum-dependent forces) is very important here. An additional argument in favor of this conclusion is that cascade simulations [38,45,48] reproduce the proton v_2 quite successfully at 158A GeV, although still overestimating at 40A GeV.

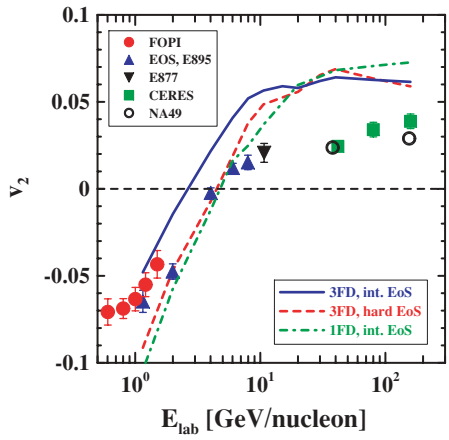

FIG. 13. (Color online) Proton elliptic flow at midrapidity as a function of incident energy in mid-central Au+Au (at AGS energies) and Pb+Pb (at SPS energies) collisions. 3FD calculations with intermediate and hard EoS's, as well as 1FD calculations are presented. Compilation of experimental data is from Ref. [53].

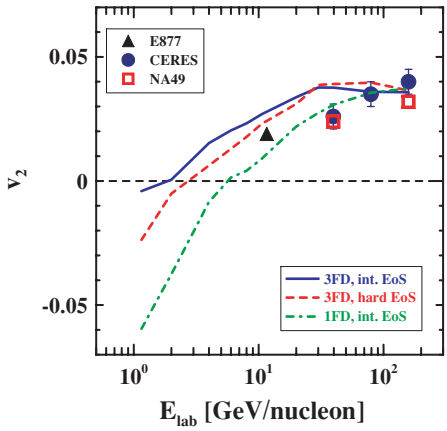

FIG. 14. (Color online) The same as in Fig. 13 but for pions.

The case of energy of 40A GeV deserves special attention. All the calculations done until now [45,51], in JAM, UrQMD, and HSD, do not reproduce the collapse of v_2 at 40A GeV, which can be interpreted as the onset of a first-order phase transition [51]. As for the 3FD model, the disagreement with the data is the largest at 40A GeV, thus also indicating that something special happens in the system at this energy.

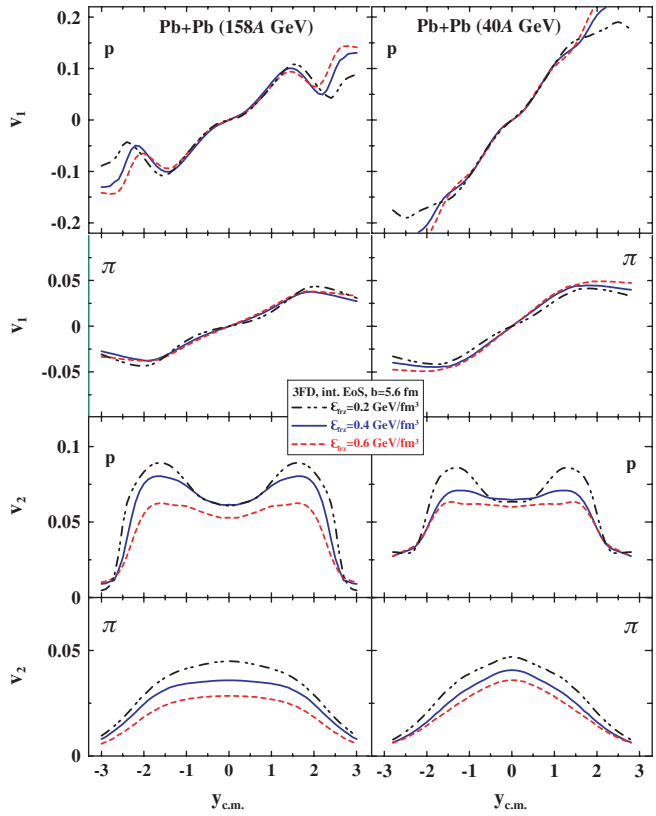

FIG. 15. (Color online) Directed (four upper panels) and elliptic (four lower panels) flow of protons and charged pions in mid-central Pb+Pb collisions at $E_{\rm lab} = 158A$ GeV (left panels) and 40A GeV (right panels) as a function of rapidity. 3FD calculations with intermediate EoS at $b = 5.6$ fm are presented for three different freeze-out criteria: the freeze-out energy density $\varepsilon_{\rm frz} = 0.2$ GeV/fm^3 (late freeze-out), $\varepsilon_{\rm frz} = 0.4$ GeV/fm^3 (our conventional freeze-out), and $\varepsilon_{\rm frz} = 0.6$ GeV/fm^3 (early freeze-out).

The earlier pion v_2 data of the NA49 collaboration, taken at smaller acceptance at the top SPS energy [60], have been already analyzed within hydrodynamic approaches. In the expansion model [89] the Bjorken scaling solution [90] was assumed for longitudinal evolution, and 2D hydro was solved numerically for transverse one. In this way the elliptic flow could be estimated only at the midrapidity point. The full 3D expansion model with postulated initial conditions was applied to the meson elliptic flow by Hirano [46]. In a qualitative agreement with Ref. [89], it was found that ρ-meson decays result in almost vanishing azimuthal anisotropy of pions near the midrapidity. Note that decays of all relevant resonances are taken into account in our model.

Figures 13 and 14 summarize our results on v_2. In addition they show that v_2 becomes less sensitive not only to the stiffness of the EoS but also to the nuclear stopping power at high incident energies. Indeed, the 1FD results become very similar to that of the 3FD model,[1] especially for protons. However, all these results overestimate the proton v_2 at high incident energies. As is seen, the 3FD with hard EoS and 1FD properly reproduce the change of sign of proton v_2. Unfortunately, data on pion v_2 are practically absent at AGS energies.

V. DISCUSSION AND CONCLUSIONS

In this paper we presented the an analysis of the collective transverse flow of nuclear matter within the 3FD model [3,13]. This is not a dedicated study of flow, aiming to reproduce experimental data by fitting model parameters. On the contrary, we have used model parameters of our previous paper [3], which were fixed to reproduce a great body of experimental data in the incident energy range $E_{\rm lab} \simeq (1\text{–}160)A$ GeV. We have varied these parameters only to study the sensitivity of the flow to stiffness of the EoS and to the nuclear stopping power.

This paper, as well as the previous one [3], is based on a simple purely hadronic EoS [14]. We do not expect that this EoS perfectly reproduces all the data (and, in fact, it does not). However, we believe that some useful conclusions can be drawn from success or failures of simulations based on this simple EoS.

At the AGS energies the flow turns out to be sensitive to the stopping power of nuclear matter rather than only to the stiffness of the EoS. The stronger the stopping power is, the harder the dynamics is; i.e., it looks as if a harder EoS were employed. This was demonstrated by comparing the 3FD and 1FD calculations.

When the stopping power is fixed to reproduce other observables, the flow data favor a softer and softer EoS with the incident energy rise. This EoS softening occurs in the AGS energy range; at higher (SPS) energies the same extrasoft EoS

[1]Note, however, that the 1FD results are completely unreasonable for other observables at high incident energies.

remains preferable. This observation indirectly agrees with that obtained in microscopic RQMD [47], UrQMD [48], JAM [45] and HSD [51] models. In these models an effective softening of the EoS occurs at the early stage of the collision because of gradual (governed by form-factors) [51] or abrupt [48] switching off of mean-field interactions, or since mean fields turn out to be essentially reduced because of string formation [45,47]. With the incident energy rise, string excitations and mean-field switching off result in progressing softening of the EoS. With this mechanism of effective softening these models efficiently reproduce the directed flow in the whole incident-energy range with the same mean-field interaction. Since the mean-field switching off is accompanied by dominating string excitations in models also [48,51], it is possible to summarize this mechanism as "a transition from hadronic to string matter," following Ref. [40]. Moreover, as was stated in Ref. [40], the transition from hadronic to string matter practically saturates at the top AGS energy. This also is in agreement with our observation that no extra softening of the EoS is required at SPS energies, as compared with the top AGS energy.

We have also found that it is impossible to reproduce the directed and elliptic flow simultaneously with the same EoS. The directed flow requires a softer EoS, while the elliptic flow demands a harder EoS. This observation is similar to that done in Refs. [24,44]. In Refs. [43,45] it was found that a proper momentum dependence in the nuclear mean field is of prime importance for the simultaneous reproduction of the directed and elliptic flows. The fact that this momentum dependence is vitally important apparently suggests that the initial stage of nuclear collision (i.e., the formation of a so-called initial fireball) is essentially nonequilibrium and that the flow is sensitive to this early nonequilibrium in the transverse-momentum distribution.

At SPS energies the directed-flow data favor the same extrasoft EoS that was the best beginning from the incident energy of 8A GeV. This EoS softening can be associated with either the transition from hadronic to string matter [40], which has been mentioned already, or could be a signal of deconfinement transition. Within the 3FD simulations the elliptic flow becomes less sensitive to the stiffness of the EoS and even to the stopping power at these energies. Lack of the proper description of the nonequilibrium transverse-momentum anisotropy at the initial stage of nuclear collision prevents the 3FD from good reproduction of the proton elliptic flow at SPS energies. Disagreement of the 3FD with the data is largest at 40A GeV incident energy, which may indicate that something special happens in the system at this energy.

The above discussion suggests that the flow is an early-stage observable, i.e., that determined by early-stage evolution of the collision. Our calculations with different freeze-out criteria (different freeze out energy densities $\varepsilon_{\rm frz}$), displayed in Fig. 15 confirm this conjecture. From the point of view of freeze out, the difference between $\varepsilon_{\rm frz} = 0.2$ and 0.6 GeV/fm^3 is huge—they correspond to completely different patterns of freeze out. Nevertheless, the directed flow turns out to be fairly insensitive to this difference. Slight sensitivity is observed only in spectator regions. The elliptic flow is a more subtle quantity. It is a measure of the difference of the in-plane and out-of-plane flow. Taking into account that our calculated v_2 are of the order of 5% and that sensitivity of v_1 with respect to the above $\varepsilon_{\rm frz}$ variations is $\approx$1%, the value of 20% for the variation of v_2 under the above change of $\varepsilon_{\rm frz}$ looks quite natural. In fact, this low sensitivity of the flow to the freeze-out stage is not surprising. The v_1 flow is a measure of collective momentum accumulated by matter during the expansion stage. The driving force of this collective momentum is the pressure gradient created at the early compression stage of the collision. If the freeze-out occurs not too early (e.g., not right after the compression stage), this pressure gradient has enough time to accelerate the matter, and hence late-stage evolution does not noticeably change the earlier-accumulated collective momentum.

Thus, problems in reproduction of flow data apparently result from a not quite accurate description of early-stage transverse-momentum nonequilibrium within the 3FD rather than resulting from our intermediate hadronic EoS. Therefore, keeping in mind that with our intermediate hadronic EoS we have succeeded in reasonably reproducing a large body of experimental data in the incident energy range $E_{\rm lab} \simeq$ (1–160)A GeV [3], we can still conclude that this EoS is certainly good (however, not perfect) in this energy range. However, since the required EoS softening can be still associated with a deconfinement transition, other, more sophisticated EoS's, including the phase transition to the quark-gluon phase, should be tested within 3FD simulations. The present calculations provide a natural benchmark for future analysis.

ACKNOWLEDGMENTS

We are grateful to M. Gazdzicki, V. V. Skokov, V. D. Toneev, and D. N. Voskresensky for fruitful discussions. This work was supported in part by the Deutsche Forschungsgemeinschaft (DFG project 436 RUS 113/558/0-3), the Russian Foundation for Basic Research (RFBR grant 06-02-04001 NNIO_a), and the Russian Federal Agency for Science and Innovations (grant NSh-8756.2006.2).

APPENDIX A: HADRONIC EOS

The EoS used in the present simulations was originally proposed in Ref. [14]. The energy density and pressure are constructed as follows:

$$\varepsilon(n_B, T) = \varepsilon_{\rm gas}(n_B, T) + W(n_B), \tag{A1}$$

$$P(n_B, T) = P_{\rm gas}(n_B, T) + n_B \frac{dW(n_B)}{dn_B} - W(n_B), \tag{A2}$$

where $\varepsilon_{\rm gas}(n_B, T)$ and $P_{\rm gas}(n_B, T)$ are the energy density and pressure of relativistic hadronic gas, respectively, which depend on baryon density n_B and temperature T. The only difference from the ideal gas is that baryons are affected by a mean field $U(n_B) = dW(n_B)/dn_B$; i.e., the energy of the a baryon of mass M_a with momentum $\mathbf{p}$ is $\epsilon_a = (\mathbf{p}^2 + M_a^2)^{1/2} + b_a U(n_B)$, where b_a is the baryon number of the a particle. The potential energy density $W(n_B)$ is parametrized

as follows:

$$W(n_B) + \varepsilon_{\rm gas}(n_B, 0) = m_N n_0 \left[a \left(\frac{n_B}{n_0}\right)^{5/3} - b \left(\frac{n_B}{n_0}\right)^{2} + c \left(\frac{n_B}{n_0}\right)^{7/3} \right], \quad \text{(A3)}$$

where $\varepsilon_{\rm gas}(n_B, 0)$ is the Fermi energy density of the cold nucleon gas.[2] This potential energy density depends only on the density n_B. Parameters a, b, and c are determined from the condition that the cold nuclear matter saturates at $n_0 = 0.15\ \text{fm}^{-3}$ and $\varepsilon(n_0, T = 0)/n_0 - m_N = -16$ MeV, and the incompressibility of this nuclear matter is K. Typically we use the value $K = 210$ MeV (intermediate EoS). However, some calculations are also done for $K = 380$ MeV (hard EoS), $K = 130$ MeV (soft EoS), and $K = 100$ MeV (extrasoft EoS).

Parametrization (A3) results in a superluminal sound velocity at high baryon densities. To preserve causality at high n_B, the form of the energy density used is

$$\varepsilon(n_B, T=0) = n_0 m_N \left[A \left(\frac{n_B}{n_0}\right)^{2} + C + B \left(\frac{n_0}{n_B}\right) \right] \quad \text{(A4)}$$

at $n_B/n_0\ \chi_c$. Parameters A, B, and C are determined under the condition that $\varepsilon(n_B, T = 0)$, and its two first derivatives are continuous at $n_B/n_0 = x_c$. The baryon density, where parametrization (A4) starts, depends on the incompressibility K: $x_c = 6$ for our basic intermediate EoS, $x_c = 5$ for the hard EoS, and $x_c = 12$ for the soft EoS. Parametrization (A3) for the extrasoft EoS does not violate causality at the considered densities.

[2]This Fermi energy density is present here because in fact we parametrized the zero-temperature part of the energy density, $\varepsilon(n_B, 0)$.

[1] B. Friman, W. Nörenberg, and V. D. Toneev, Eur. Phys. J. A **3**, 165 (1998).
[2] W. Cassing and E. L. Bratkovskaya, Phys. Rep. **308**, 65 (1999).
[3] Yu. B. Ivanov, V. N. Russkikh, and V. D. Toneev, Phys. Rev. C **73**, 044904 (2006).
[4] M. Gazdzicki and M. I. Gorenstein, Acta Phys. Pol. B **30**, 2705 (1999).
[5] P. Braun-Munzinger, J. Cleymans, H. Oeschler, and K. Redlich, Nucl. Phys. **A697**, 902 (2002).
[6] M. Gazdzicki *et al.* (NA49 Collaboration), J. Phys. G **30**, S701 (2004).
[7] M. Asakawa and K. Yazaki, Nucl. Phys. **A504**, 668 (1989).
[8] Z. Fodor and S. D. Katz, J. High Energy Phys. 03 (2002) 14; 04 (2004) 50.
[9] M. Stephanov, K. Rajagopal, and E. Shuryak, Phys. Rev. D **60**, 114028 (1999).
[10] FAIR "An International Accelerator Facility for Beams of Ions and Antiprotons," http://www.gsi.de/fair/.
[11] N. Antoniou *et al.*, CERN-SPSC-2006-001, CERN-SPSC-P-329 (Letter of Intent of NA49-Future Collaboration).
[12] A. Cho, Science **312**, 190 (2006).
[13] V. D. Toneev, Yu. B. Ivanov, E. G. Nikonov, W. Norenberg, and V. N. Russkikh, Phys. Part. Nucl. Lett. **2**, 288 (2005) [Pi'ma o Fizike Elementarnykh Chastits i Atomnogo Yadra **2**, 43 (2005)]; V. N. Russkikh, Yu. B. Ivanov, E. G. Nikonov, W. Norenberg, and V. D. Toneev, Phys. At. Nucl. **67**, 199 (2004) [Yad. Fiz. **67**, 195 (2004)].
[14] V. M. Galitsky and I. N. Mishustin, Sov. J. Nucl. Phys. **29**, 181 (1979).
[15] W. Cassing and U. Mosel, Prog. Part. Nucl. Phys. **25**, 235 (1990).
[16] H. Stöcker and W. Greiner, Phys. Rep. **137**, 277 (1986).
[17] H. H. Gutbrod, A. M. Poskanzer, and H. G. Ritter, Rep. Prog. Phys. **52**, 1267 (1989).
[18] C. Gale, G. M. Welke, M. Prakash, S. J. Lee, and S. Das Gupta, Phys. Rev. C **41**, 1545 (1990).
[19] J. Zhang, S. Das Gupta, and C. Gale, Phys. Rev. C **50**, 1617 (1994).
[20] V. N. Russkikh and Yu. B. Ivanov, Nucl. Phys. **A591**, 699 (1995).
[21] M. D. Partlan *et al.* (EOS Collaboration), Phys. Rev. Lett. **75**, 2100 (1995).
[22] N. Herrmann *et al.* (FOPI Collaboration), Nucl. Phys. **A610**, 49c (1996).
[23] J. Chance *et al.* (EOS Collaboration), Phys. Rev. Lett. **78**, 2535 (1997).
[24] P. Danielewicz, R. A. Lacey, P.-B. Gossiaux, C. Pinkenburg, P. Chung, J. M. Alexander, and R. L. McGrath, Phys. Rev. Lett. **81**, 2438 (1998); P. Danielewicz, Nucl. Phys. **A673**, 34 (2000); P. Danielewicz, Nucl. Phys. **A685**, 368 (2001).
[25] J.-Y. Ollitrault, Phys. Rev. D **46**, 229 (1992); H. Sorge, Phys. Rev. Lett. **78**, 2309 (1997).
[26] W. Reisdorf and H. G. Ritter, Annu. Rev. Nucl. Part. Sci. **47**, 1 (1997).
[27] P. Braun-Munzinger and J. Stachel, Nucl. Phys. **A638**, 3c (1998).
[28] Q. Pan and P. Danielewicz, Phys. Rev. Lett. **70**, 2062 (1993).
[29] T. Maruyama, W. Cassing, U. Mosel, S. Teis, and K. Weber, Nucl. Phys. **A573**, 653 (1994).
[30] D. Rischke, Nucl. Phys. **A610**, 88c (1996).
[31] S. A. Bass *et al.*, Prog. Part. Nucl. Phys. **41**, 225 (1998); J. Phys. G **25**, R1 (1999).
[32] S. K. Ghosh, S. C. Phatak, and P. K. Sahu, Z. Phys. A **352**, 457 (1996).
[33] B.-A. Li, C. M. Ko, A. T. Sustich, and B. Zhang, Phys. Rev. C **60**, 011901(R) (1999).
[34] J. Brachmann, S. Soff, A. Dumitru, H. Stöcker, J. A. Maruhn, W. Greiner, L. V. Bravina, and D. H. Rischke, Phys. Rev. C **61**, 024909 (2000).
[35] A. Hombach, W. Cassing, S. Teis, and U. Mosel, Eur. Phys. J. A **5**, 157 (1999).
[36] Y. Nara, N. Otuka, A. Ohnishi, and T. Maruyama, Prog. Theor. Phys. Suppl. **129**, 33 (1997).
[37] M. Belkacem, M. Brandstetter, S. A. Bass *et al.*, Phys. Rev. C **58**, 1727 (1998); L. V. Bravina *et al.*, J. Phys. G **25**, 351 (1999).
[38] L. V. Bravina, A. Faessler, C. Fuchs, and E. E. Zabrodin, Phys. Rev. C **61**, 064902 (2000).
[39] P. K. Sahu, A. Hombach, W. Cassing, M. Effenberger, and U. Mosel, Nucl. Phys. **A640**, 493 (1998).
[40] P. K. Sahu, W. Cassing, U. Mosel, and A. Ohnishi, Nucl. Phys. **A672**, 376 (2000).
[41] A. B. Larionov, W. Cassing, C. Greiner, and U. Mosel, Phys. Rev. C **62**, 064611 (2000).

[42] Yu. B. Ivanov, E. G. Nikonov, W. Nörenberg, V. D. Toneev, and A. A. Shanenko, Heavy Ion Phys. **15**, 117 (2002).
[43] P. K. Sahu and W. Cassing, Nucl. Phys. **A712**, 357 (2002).
[44] P. Danielewicz, R. Lacey, and W. G. Lynch, Science **298**, 1592 (2002); P. Danielewicz, arXiv.org:nucl-th/0512009.
[45] M. Isse, A. Ohnishi, N. Otuka, P. K. Sahu, and Y. Nara, Phys. Rev. C **72**, 064908 (2005).
[46] T. Hirano, Phys. Rev. Lett. **86**, 2754 (2001).
[47] H. Liu, S. Panitkin, and N. Xu, Phys. Rev. C **59**, 348 (1999).
[48] S. Soff, S. A. Bass, M. Bleicher, H. Stoecker, and W. Greiner, arXiv.org:nucl-th/9903061.
[49] L. P. Csernai and D. Roehrich, Phys. Lett. **B458**, 454 (1999).
[50] E. E. Zabrodin, C. Fuchs, L. V. Bravina, and A. Faessler, Phys. Rev. C **63**, 034902 (2001).
[51] H. Stöcker, E. L. Bratkovskaya, M. Bleicher, S. Soff, and Z. Zhu, J. Phys. G **31**, S929 (2005).
[52] C. M. Hung and E. V. Shuryak, Phys. Rev. Lett. **75**, 4003 (1995).
[53] A. Andronic *et al.* (FOPI Collaboration), Phys. Lett. **B612**, 173 (2005).
[54] P. Chung *et al.* (E895 Collaboration) and P. Danielewicz, Phys. Rev. C **66**, 021901(R) (2002).
[55] J. Barrette *et al.* (E877 Collaboration), Phys. Rev. C **55**, 1420 (1997); **56**, 3254 (1997).
[56] K. Filimonov *et al.* (E877 Collaboration), Nucl. Phys. **A661**, 198 (1999).
[57] C. Pinkenburg *et al.* (E895 Collaboration), Phys. Rev. Lett. **83**, 1295 (1999).
[58] H. Liu *et al.* (E895 Collaboration), Phys. Rev. Lett. **84**, 5488 (2000).
[59] J. L. Klay *et al.* (E895 Collaboration), Phys. Rev. Lett. **88**, 102301 (2002).
[60] H. Appelshäuser *et al.* (NA49 Collaboration), Phys. Rev. Lett. **80**, 4136 (1998).
[61] H. Appelshäuser *et al.* (NA49 Collaboration), Phys. Rev. Lett. **82**, 2471 (1999).
[62] C. Alt *et al.* (NA49 Collaboration), Phys. Rev. C **68**, 034903 (2003).
[63] K. Filimonov *et al.* (CERES Collaboration), arXiv.org:nucl-ex/0109017; J. Slivova (CERES Collaboration), Nucl. Phys. **A715**, 615c (2003).
[64] Y. Nara, N. Otuka, A. Ohnishi, K. Niita, and S. Chiba, Phys. Rev. C **61**, 024901 (2000).
[65] T. Maruyama *et al.*, Prog. Theor. Phys. **96**, 263 (1996).
[66] I. N. Mishustin, V. N. Russkikh, and L. M. Satarov, Yad. Fiz. **48**, 711 (1988) [Sov. J. Nucl. Phys. **48**, 454 (1988)]; Nucl. Phys. **A494**, 595 (1989); Yad. Fiz. **54**, 429 (1991) [Sov. J. Nucl. Phys. **54**, 260 (1991)].
[67] V. N. Russkikh, Yu. B. Ivanov, Yu. E. Pokrovsky, and P. A. Henning, Nucl. Phys. **A572**, 749 (1994).
[68] Yu. B. Ivanov, V. N. Russkikh, M. Schönhofen, M. Cubero, B. L. Friman, and W. Nörenberg, Z. Phys. A **340**, 385 (1991); Yu. B. Ivanov and V. N. Russkikh, Nucl. Phys. **A580**, 614 (1994); Yad. Fiz. **58**, 2180 (1995) [Phys. At. Nucl. **58**, 2066 (1995)]; Yad. Fiz. **60**, 743 (1997) [Phys. At. Nucl. **60**, 660 (1997)]; S. Ayik, Yu. B. Ivanov, V. N. Russkikh, and W. Nörenberg, Nucl. Phys. **A578**, 640 (1994).
[69] U. Katscher, D. H. Rischke, J. A. Maruhn, W. Greiner, I. N. Mishustin, and L. M. Satarov, Z. Phys. A **346**, 209 (1993); A. Dumitru, U. Katscher, J. A. Maruhn, H. Stöcker, W. Greiner, and D. H. Rischke, Phys. Rev. C **51**, 2166 (1995); Z. Phys. A **353**, 187 (1995).
[70] J. Brachmann, A. Dumitru, J. A. Maruhn, H. Stöcker, W. Greiner, and D. H. Rischke, Nucl. Phys. **A619**, 391 (1997); M. Reiter, A. Dumitru, J. Brachmann, J. A. Maruhn, H. Stöcker, and W. Greiner, Nucl. Phys. **A643**, 99 (1998); M. Bleicher, M. Reiter, A. Dumitru, J. Brachmann, C. Spieles, S. A. Bass, H. Stöcker, and W. Greiner, Phys. Rev. C **59**, R1844 (1999); J. Brachmann, A. Dumitru, H. Stöcker, and W. Greiner, Eur. Phys. J. A **8**, 549 (2000).
[71] L. M. Satarov, Yad. Fiz. **52**, 412 (1990) [Sov. J. Nucl. Phys. **52**, 264 (1990)].
[72] T. Klahn *et al.*, arXiv.org:nucl-th/0602038.
[73] A. Andronic, P. Braun-Munzinger, and J. Stachel, arXiv.org:nucl-th/0511071.
[74] J. Barrette *et al.* (E877 Collaboration), Phys. Rev. C **51**, 3309 (1995).
[75] J. L. Klay *et al.* (E895 Collaboration), Phys. Rev. C **68**, 054905 (2003).
[76] L. Ahle *et al.* (E866 and E917 Collaborations), Phys. Lett. **B476**, 1 (2000); **B490**, 53 (2000); B. B. Back *et al.* (E917 Collaboration), Phys. Rev. Lett. **86**, 1970 (2001).
[77] S. V. Afanasiev *et al.* (NA49 Collaboration), Phys. Rev. C **66**, 054902 (2002); V. Friese *et al.* (NA49 Collaboration), J. Phys. G **30**, S119 (2004); C. Alt *et al.* (NA49 Collaboration), arXiv.org:nucl-ex/0512033.
[78] I. G. Bearden *et al.* (NA44 Collaboration), Phys. Rev. C **66**, 044907 (2002).
[79] F. Antinori *et al.* (NA57 Collaboration), J. Phys. G **31**, 1345 (2005).
[80] C. Pinkenburg *et al.* (E895 Collaboration), Nucl. Phys. **A698**, 495 (2002).
[81] B. B. Back *et al.* (E917 Collaboration), Phys. Rev. Lett. **87**, 242301 (2001).
[82] T. Anticic *et al.* (NA49 Collaboration), Phys. Rev. Lett. **93**, 022302 (2004).
[83] P. Danielewicz and G. Odyniec, Phys. Lett. **B157**, 146 (1985).
[84] S. Voloshin and Y. Zhang, Z. Phys. C **70**, 665 (1996).
[85] A. M. Poskanzer and S. A. Voloshin, Phys. Rev. C **58**, 1671 (1998).
[86] N. Borghini, P. M. Dinh, and J. Y. Ollitrault, Phys. Rev. C **63**, 054906 (2001); **64**, 054901 (2001); **66**, 014905 (2002).
[87] S. A. Bass, R. Mattiello, H. Stöcker, W. Greiner, and Ch. Hartnack, Phys. Lett. **B302**, 381 (1993).
[88] B.-A. Li, Nucl. Phys. **A571**, 797 (1994).
[89] J. P. Kolb, J. Sollfrank, and U. Heinz, Phys. Lett. **B459**, 667 (1999).
[90] J. D. Bjorken, Phys. Rev. D **27**, 140 (1983).